

# Bright cavity polariton solitons

O.A. Egorov<sup>1</sup>, D.V. Skryabin<sup>2</sup>, A.V. Yulin<sup>2</sup> and F. Lederer<sup>1</sup>

<sup>1</sup>*Institute of Condensed Matter Theory and Solid State Optics,  
Friedrich-Schiller-Universität Jena, Max-Wien-Platz 1, 07743 Jena, Germany*

<sup>2</sup>*Centre for Photonics and Photonic Materials, Department of Physics,  
University of Bath, Bath BA2 7AY, United Kingdom*

(Dated: October 31, 2018)

The lower branch of the dispersion relation of exciton polaritons in semiconductor microcavities, operating in the strong-coupling regime, contains sections of both positive and negative curvature along one spatial direction. We show that this leads to the existence of stable one-dimensional bright microcavity solitons supported by the repulsive polariton nonlinearity. To achieve localization along the second transverse direction we propose to create a special soliton waveguide by changing the cavity detuning and hence the boundary of the soliton existence in such a way that the solitons are allowed only within the stripe of the desired width.

The study of nonlinear and quantum effects in optical microcavities is an area of current vigorous activity [1, 2, 3]. In particular, the strong coupling regime in quantum well semiconductor microcavities [1, 2] leads to a strong and fast nonlinear response of microcavity exciton polaritons, which have been used for low threshold bistability [4, 5, 6, 7], parametric wave mixing [8, 9, 10, 11, 12, 13] and for the demonstration of long range polariton coherence supporting claims for observation of Bose-Einstein condensation [14, 15, 16, 17, 18, 19]. Research in this area bordering condensed matter physics and photonics has links with many topics of current interest, which include, but not limited to, superfluidity, solitons, vortices, photonic crystals and quantum information.

Diffraction and dispersion are important features of waves of any nature and the problem of their control stimulates significant research efforts. The recent time has witnessed remarkable developments into photonic crystals, which can be used to fully compensate diffraction and to control its value and sign, see, e.g., [20, 21]. The ideas developed for electromagnetic waves have also been applied to matter waves [22], surface plasmons [23] and other waves. Microcavity polaritons have been a part of these research efforts, with periodic potentials for polaritons created by the mirror patterning or by the surface acoustic waves [24, 25]. Note, that the term diffraction is most commonly used when the beam spreading happens upon propagation in space. While, in the context of planar microcavities one deals with the temporal evolution of spots of light, which is analogous to the spreading of quantum wave packets. This evolution is governed by the dispersion law linking the frequency (or energy) to the transverse wavenumber (or momentum).

Diffraction and dispersion control has been comprehensively discussed and used in conjunction with spatial and temporal soliton formation, see e.g. [26, 27, 28]. A particular field of these studies concerns spatial cavity solitons in the weak coupling regime with periodic modulation of the detuning and/or other cavity parameters, see, e.g., [29]. Weak and strong coupling regime differ mainly in that in the latter case the dispersion curve ex-

hibits two branches signalling mixing of light and matter excitations. Namely, additionally to the upper parabolic branch, which is largely a photonic one, the lower polariton branch appears. In our context the most relevant feature is that this lower branch exhibits an inflection point where the second order dispersion changes sign [Fig.1(a)]. It is worth noting that this effect is merely evoked by the strong photon-exciton coupling, hence it appears even in a homogeneous cavity and does not require any modulation as in the weak coupling regime. The primary goal of this Letter is to demonstrate how this peculiarity can be exploited for the formation of stable *bright* cavity polariton solitons (CPSs) supported by the repulsive exciton-exciton interaction. However, the inflection of the dispersion curve provides only localization in one dimension and additional measures for soliton trapping in the other dimension have to be implemented relying on the soliton existence domain shift by means of the space dependent detuning control.

Recently it has been suggested to use bright cavity solitons in the *weak* coupling regime in all optical processing schemes [30, 31, 32]. In this context bright CPSs in the *strong* coupling regime are superior and promising candidates for a practical implementation because they have a picosecond excitation time and require extremely low pump intensities of about 100 W/cm<sup>2</sup>, thus surpassing their weakly coupled counterparts by almost two orders of magnitude on these two crucial parameters [33]. The first experimental observations of dark and bright soliton-like structures in the strong coupling regime of semiconductor microcavities have been recently reported in [34] calling for more theoretical and experimental studies of this topic. It has been demonstrated [33] that the dark solitons are the only stable solutions with momenta centered around the bottom of the lower polariton branch.

The widely accepted dimensionless model for excitons strongly coupled to cavity photons is [1, 2, 6, 33]

$$\begin{aligned} \partial_t E - i(\partial_x^2 + \partial_y^2)E + [\gamma_c - i\Delta - iU(y)] E &= \\ = i\Psi + E_0 e^{ik_0 x}, & \\ \partial_t \Psi + (\gamma_0 - i\Delta)\Psi + i|\Psi|^2 \Psi = iE. & \end{aligned} \quad (1)$$

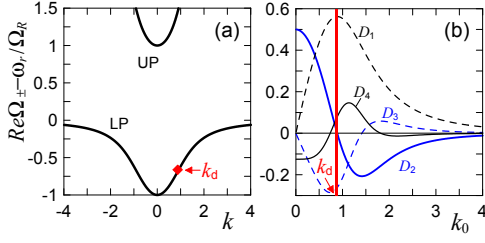


FIG. 1: (color online) (a) Polariton dispersion: lower (LP) and upper (UP) branch in the strong coupling regime. (b) Dispersion coefficients vs. inclination of the holding beam  $k_0$ .

Here  $E$  and  $\Psi$  are the averages of the photon and exciton creation or annihilation operators and polarization effects are disregarded. The normalization is such that  $(\Omega_R/g)|E|^2$  and  $(\Omega_R/g)|\Psi|^2$  are the photon and exciton numbers per unit area. Here,  $\Omega_R$  is the Rabi frequency and  $g$  is the exciton-exciton interaction constant.  $\Delta = (\omega - \omega_r)/\Omega_R$  describes detuning of the pump frequency  $\omega$  from the identical resonance frequencies of excitons and cavity,  $\omega_r$ . The time  $t$  is measured in units of  $1/\Omega_R$ .  $\gamma_c$  and  $\gamma_0$  are the cavity and exciton damping constants normalized to  $\Omega_R$ . The transverse coordinates  $x$ ,  $y$  are normalized to the value  $x_0 = \sqrt{c/2k_z n \Omega_R} \sim 1 \mu\text{m}$  where  $c$  is the vacuum light velocity,  $n$  is the refractive index and  $k_z = n\omega/c$  is the wavenumber. The normalized amplitude of the external pump  $E_0$  is related to the physical incident intensity  $I_{inc}$  as  $|E_0|^2 = g\gamma_c I_{inc}/\hbar\omega_0\Omega_R^2$  [13].  $k_0$  is the transverse wavenumber of the pump, with  $k_0 = 0$  corresponding to normal incidence. As a guideline for realistic estimates one can use parameters of a microcavity with a single InGaAs/GaAs quantum well:  $\hbar\Omega_R \simeq 2.5$  meV,  $\hbar g \simeq 10^{-4}$  eV $\mu\text{m}^2$ , see [5, 6]. Assuming the relaxation times of the photonic and excitonic fields to be 2.5 ps gives  $\gamma_{c,0} \simeq 0.1$ . In accordance with this set of parameters the normalized driving amplitude  $|E_0|^2 = 1$  corresponds to an external pump intensity of about 10 kW/cm<sup>2</sup>. Optical bistability appears for  $|E_p| \sim 0.1$  or about 10<sup>2</sup>–10<sup>3</sup>W/cm<sup>2</sup>.  $U(y)$  is the spatially varying shift of the cavity resonance which represents a potential for photons. The spatial inhomogeneities of the cavity and quantum wells are assumed negligible, so that long range spatial effects can be observed. As, for example, in the recent demonstration of the 50 $\mu\text{m}$  in diameter anti-phase polariton  $\pi$ -state in a microcavity with periodically patterned mirrors [24].

To understand the physics of CPS formation and to identify domains of their existence we first expand the linear polariton dispersion around the pump wavevector, and arrive after an inverse Fourier transformation at a single equation with an effective nonlinearity and multiple dispersion terms. We assume  $U = 0$  and look for the linear polariton eigenstates, i.e., the photons trapped in the pump free cavity ( $E_0 = 0$ ,  $\Delta \rightarrow -\omega_r/\Omega_R$ ) coupled to noninteracting excitons. Seeking solutions of Eqs. (1) in the form  $E, \Psi = e_k, \psi_k e^{-i\Omega t + ikx}$  gives the eigenvalue

problem:

$$i\Omega_{\pm}(k)\vec{p}_k = \begin{pmatrix} ik^2 + \gamma_c + i\omega_r/\Omega_R & -i \\ -i & \gamma_0 + i\omega_r/\Omega_R \end{pmatrix} \vec{p}_k, \quad (2)$$

where  $\vec{p}_k = \{e_k, \psi_k\}$  is the polariton basis vector and  $\Omega_{\pm}(k)$  are the eigenfrequencies, corresponding to the upper- (+) and lower- (-) branch of the polariton dispersion curve, respectively, see Fig. 1. The inflection point  $\partial_k^2 \Omega_- = 0$  is located at  $k = k_d$ , where second order dispersion disappears.

The standard next step here would be to disregard the upper branch and to consider the  $k_0$  values close to zero, see, e.g. [1, 2, 5, 6]. In order to embrace the inflection point and to account for the varying dispersion we modify this technique and include higher-order dispersion terms. To achieve this we perform the Fourier transform  $\{E, \Psi\} \simeq \int a(t, k)\vec{p}_k e^{ikx} dk$ , where  $a(t, k)$  is the Fourier amplitude of the  $k$ -th component and  $\vec{p}_k$  corresponds to the lower polariton branch. We assume that the spectrum of the polariton wavepacket is centered around  $k_0$  and expand  $\Omega_-(k)$  up to the fourth order in  $|k - k_0|$ . The slowly varying amplitude of the polariton wavepacket is then  $A(t, x) = \int_{-\infty}^{\infty} a(t, k) e^{i(k-k_0)x} d(k - k_0)$  and obeys:

$$i\partial_t A + iD_1 \partial_x A + D_2 \partial_x^2 A - iD_3 \partial_x^3 A - D_4 \partial_x^4 A - \delta A - \xi |A|^2 A = i\eta E_0, \quad (3)$$

where  $\delta = \Omega_-(k_0) - \omega/\Omega_R$ ,  $\text{Re } \delta$  is the polariton detuning from the pump frequency and  $\text{Im } \delta$  is the loss.  $D_1 = \partial_k \Omega_-|_{k_0}$  is the transverse group velocity and  $D_2 = (1/2)\partial_k^2 \Omega_-|_{k_0}$ ,  $D_3 = (1/6)\partial_k^3 \Omega_-|_{k_0}$ ,  $D_4 = (1/24)\partial_k^4 \Omega_-|_{k_0}$  are the dispersion coefficients [Fig. 1(b)].  $\xi = |\psi_{k_0}|^4 / (|e_{k_0}|^2 + |\psi_{k_0}|^2)$  is the effective nonlinearity and  $\eta = e_{k_0} / (|e_{k_0}|^2 + |\psi_{k_0}|^2)$ . For  $k_0$  varying from zero and towards, (but not too close to  $k_d$ )  $D_2 > 0$  dominates over  $D_{m>2}$  [Fig. 1(b)]. In this case Eq. (3) coincides with the well-known weak-coupling Lugiato-Lefever (LL) model [35].

In the LL models applied for the lower polaritons the dispersion is always normal,  $D_2 > 0$ , and the nonlinearity is repulsive, therefore the only stable CPSs are the dark ones [33], while bright solitons exist, but are unstable [Fig. 2(a,b)]. However,  $D_2(k)$  crosses zero at  $k_0 = k_d$  and the  $D_3$ -term becomes the leading one around this point. Then the  $D_3$ -term drops and the polariton dispersion is determined by the competing  $D_2$  and  $D_4$  terms. Both  $D_2 < 0$  and  $D_4 > 0$  favor the existence of bright solitons for the repulsive nonlinearity and therefore we expect to find them for  $k_0 > k_d$ . Moreover, it is evident that because of  $D_1 \neq 0$  these solitons are forced to move.

While the above considerations are useful for qualitative understanding, we return to the original model (1) with  $\partial_y = 0$  in order to compute 1D bright CPSs. In seeking for soliton solutions we have to take their motion into account:  $E(t, x) = \tilde{E}(\xi) e^{ik_0 x}$ ,  $\Psi(t, x) = \tilde{\Psi}(\xi) e^{ik_0 x}$ ,  $\xi = x - vt$ , where  $v$  is the velocity (yet to be determined) close, but not equal, to  $D_1$ , see Fig. 2(a).  $\tilde{E}$  and  $\tilde{\Psi}$

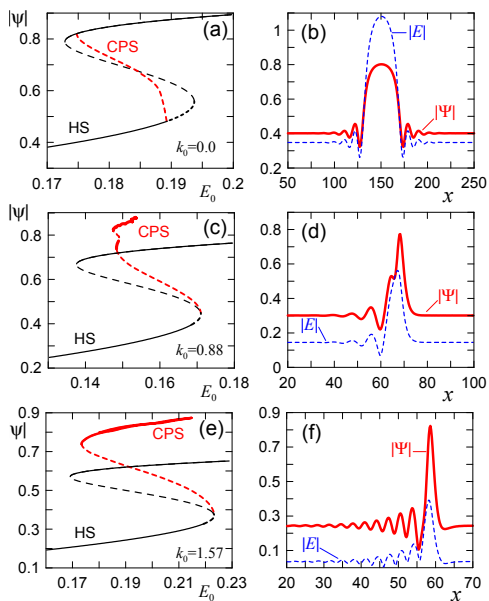


FIG. 2: (color online) Maxima of the excitonic components of the solitons vs  $E_0$  (left column) and the soliton profiles (right column) for different  $k_0$ . Black lines in the left column mark the peak amplitudes of the spatially homogeneous solutions (HS) and the red ones of the solitons. The full/dashed lines in the left column correspond to stable/unstable solutions respectively.  $E_0$  and  $\Delta$  values are: (a,b) 0.175 and  $-0.7$ ; (c,d) 0.149 and  $-0.39$ ; (e,f) 0.19 and  $-0.05$ .

obey  $(2k_0 - v)\partial_\xi \tilde{E} - i\partial_\xi^2 \tilde{E} + (\gamma_c - i\Delta + ik_0^2)\tilde{E} = i\tilde{\Psi} + E_0$  and  $-v\partial_\xi \tilde{\Psi} + (\gamma_0 - i\Delta)\tilde{\Psi} + i|\tilde{\Psi}|^2 \tilde{\Psi} = i\tilde{E}$ . Bright CPS solutions of the above model are found by a modification of the Newton method allowing to treat  $v$  as an unknown variable. The maximum of  $v$  occurs at  $k = k_d$ , then the soliton velocity decreases with  $k_0$  increasing and approaches zero, see Fig. 3(a). This is in remarkable contrast to what happens if dispersion is parabolic, where the soliton velocity continuously increases with  $k_0$ . For our choice of parameters  $v$  must be multiplied by  $4 \times 10^6$  m/s to give the physical velocity. It implies that the CPS with  $v = 0.25$  will traverse across the typical distance of  $100 \mu\text{m}$  in 100ps. This is 40 times larger than the polariton life time. Hence, once excited, the solitons have enough time to shape and be observed during their motion.

Plots illustrating the dependence of the maximal soliton amplitude from the pump field and the associated bistability curves for the homogeneous ( $\partial_{x,y} = 0$ ) solutions are shown in the left column of Fig. 2. The right column shows the corresponding transverse soliton profiles. For  $k_0 = 0$  we are reproducing the results of [33] with bright CPSs being unstable. For  $k_0$  just below and above  $k_d$  the branch of bright CPSs starts bending and islands of their stability start to emerge and expand with  $k_0$  increasing.

To reveal the influence of different dispersion orders on the CPSs we plotted the dependence of the CPS width

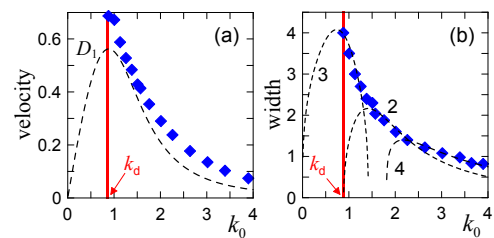


FIG. 3: (color online) (a) Diamonds show numerically computed soliton velocity vs.  $k_0$ . Dashed line shows  $D_1(k_0)$ . (b) Diamonds show the soliton width vs  $k_0$ . Dashed lines show the appropriately scaled  $\sqrt[m]{D_m}$ , where  $m = 2, 3, 4$ .

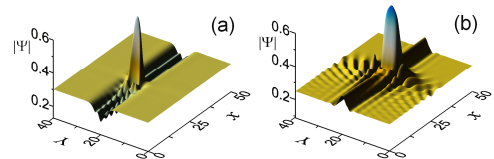


FIG. 4: (color online) (a) Soliton moving along the potential attractive for linear polaritons:  $U = b \exp[-(y/2)^8]$ ,  $b = 2$ ,  $E_0 = 0.18$ . Other parameters as in Fig. 2(e,f). (b) Soliton moving along the repulsive potential  $b = -1$ ,  $E_0 = 0.213$ .

on the inclination parameter  $k_0$  in Fig. 3(b). Since not only the dispersion coefficients vary with  $k_0$ , but also  $\text{Re } \delta$  (which strongly influences the CPS width), we have kept the latter fixed at  $\text{Re } \delta = -0.3$ , by adjusting the detuning  $\Delta$  respectively. For large  $k_0$  the excitonic part of CPSs dominates over the photonic component, see Fig. 2. That is why the CPSs can be much narrower than the pure photonic cavity solitons in the weak coupling regime and may attain widths well below the ones allowed by the photonic dispersion, although this happens at the price of oscillatory tails. The CPS width is expected to scale with the dominant dispersion coefficients as  $\sim \sqrt[m]{D_m}$  ( $m = 2, 3, 4$ ). Fig. 3(b) compares the numerically found soliton width (diamonds) with the scaling given by the different dispersion orders (dashed lines). Third-order dispersion describes well the soliton width for relatively small  $k_0$  where  $D_2 \simeq 0$ . Further inclination brings  $D_2$  on the top, while the third-order dispersion vanishes. A further increase of  $k_0$  brings fourth-order dispersion into play, which starts to compete with  $D_2$ .

In order to use CPSs as information bits, it is desirable to have them robustly localized in both transverse dimensions. However in the homogeneous cavity this is impossible to achieve, since the signs of polariton dispersion are opposite in orthogonal directions. To solve this problem we propose to shift the cavity detuning in such a way that outside the waveguide area the soliton existence conditions are not satisfied. This is particularly easy to achieve if the operating frequency is not far from the boundary of the existence domain. With this approach, it does not matter if one uses  $U(y)$ , which traps linear waves, or  $U(y)$ , which repels them. Thus using of strongly nonlinear polariton waves extends the list of

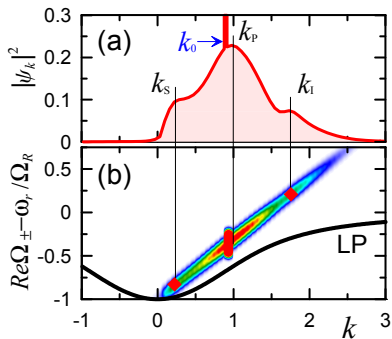


FIG. 5: (color online) (a) Excitonic part of the soliton spectrum ( $|\psi_k|$ ) of the the soliton shown in Fig. 2(d). (b) The density plot is the 2D generalization of  $|\psi_k|$  from (a). The slope of this plot shows dependence of the soliton frequency on  $k$ . The full line is LP dispersion.

the possible trapping techniques already explored for linear cavity polariton [17, 24, 36]. Fig. 4(a) demonstrates soliton guiding in the trapping potential and Fig. 4(b) in the repelling potential. The trapping potential looks preferential for the soliton guidance, because it reduces soliton interaction with the quasi-linear waves. The latter are far more pronounced in the case of the repelling potential, see Fig. 4(b). Practical excitation of CPSs is no different from their weakly coupled counterparts and requires short term application of the addressing beam in addition to the pump  $E_0$  [31, 32].

In conclusion, we have shown that stable moving 1D cavity polariton solitons exist providing the lower polaritons are used near or beyond the inflection point of their dispersion. We have also demonstrated the continuous transformation between cavity soliton polaritons shaped by the different dispersion orders, including the regimes where the influence of the usual second order dispersion is negligible. We have proposed a mechanism for their guiding and localization in the second transverse dimension. Our results form the basis for future studies of soliton-polariton logic and processing schemes.

*Note.* During the revision of this manuscript the related experimental observations of moving quasi-localised polaritons have been published [37]. Brief preliminary comparison of dispersion plots from [37] with our results is very encouraging. To reveal the soliton frequency content we take the Fourier transform of its excitonic component:  $\psi_k = \int_{-\infty}^{\infty} \tilde{\Psi}(x - vt)e^{ik_0x + ikx} dx = f(k - k_0)e^{ivt(k_0 - k)}$ , where  $f(k) = \int_{-\infty}^{\infty} \tilde{\Psi}(\xi)e^{ik\xi} d\xi$ .  $|\psi_k|$  is plotted in Fig. 5(a). Apart from the infinite peak at the at  $k_0$  corresponding to the background, the soliton spectrum proper shows 3-peak structure, such that  $2k_p = k_i + k_s$ , where  $k_p \approx k_0 \approx k_d$ . The idler field  $k_i$  was externally seeded and the signal  $k_s$  was generated in Ref. [37], while both of them are the integral parts of our soliton solution. Soliton frequency calculated from  $\psi_k$  is a straight line shifted upwards from the dispersion of linear polaritons (Fig. 5(b)). Figs. 5(a,b) essentially match the corresponding data from [37].

- 
- [1] B. Deveaud, editor. *The Physics of Semiconductor Microcavities* (Wiley-VCH, 2007).
- [2] A. Kavokin, J.J. Baumberg, G. Malpuech, and F.P. Laussy. *Microcavities* (Oxford University Press, 2007).
- [3] U. Peschel *et al.*, IEEE J. Quant. Electr. **39**, 51 (2003).
- [4] A. Tredicucci *et al.*, Phys. Rev. A **54**, 3493 (1996).
- [5] A. Baas *et al.*, Phys. Rev. A **69**, 023809 (2004).
- [6] I. Carusotto and C. Ciuti, Phys. Rev. Lett. **93**, 166401 (2004).
- [7] D. Bajoni *et al.*, Phys. Rev. Lett. **101**, 266402 (2008).
- [8] N. A. Gippius *et al.*, Europhys. Lett. **67**, 997 (2004).
- [9] D. N. Krizhanovskii *et al.*, Phys. Rev. B **77**, 115336 (2008).
- [10] R. Houdre *et al.*, Phys. Rev. Lett. **85**, 2793 (2000).
- [11] P. G. Savvidis *et al.*, Phys. Rev. Lett. **84**, 1547 (2000).
- [12] C. Diederichs *et al.*, Nature **440**, 904 (2006).
- [13] M. Wouters and I. Carusotto, Phys. Rev. B **75**, 075332 (2007).
- [14] R. M. Stevenson *et al.*, Phys. Rev. Lett. **85**, 3680 (2000).
- [15] H. Deng *et al.*, Science **298**, 199 (2002).
- [16] J. Kasprzak *et al.*, Nature **443**, 409 (2006).
- [17] R. Balili *et al.*, Science **316**, 1007 (2007).
- [18] A. P. D. Love *et al.*, Phys. Rev. Lett. **101**, 067404 (2008).
- [19] A. Baas *et al.*, Phys. Rev. Lett. **100**, 170401 (2008).
- [20] H. S. Eisenberg *et al.*, Phys. Rev. Lett. **85**, 1863 (2000).
- [21] T. Pertsch *et al.*, Phys. Rev. Lett. **88**, 093901 (2002).
- [22] B. Eiermann *et al.*, Phys. Rev. Lett. **91**, 060402 (2003);
- T. Anker *et al.*, Phys. Rev. Lett. **94**, 020403 (2005).
- [23] T. W. Ebbesen *et al.*, Nature **415**, 667 (1998).
- [24] C. W. Lai *et al.*, Nature **450**, 529 (2007).
- [25] K. Cho *et al.*, Phys. Rev. Lett. **94**, 226406 (2005).
- [26] J. W. Fleischer *et al.*, Nature **422**, 147 (2003).
- [27] Y.S. Kivshar and G. Agrawal. *Optical Solitons: From Fibers to Photonic Crystals* (Academic Press, 2001).
- [28] F. Lederer *et al.*, Phys. Rep. **463**, 1 (2008).
- [29] K. Staliunas, Phys. Rev. Lett. **91**, 053901 (2003); D. Gomila, R. Zambrini, and G. L. Oppo, Phys. Rev. Lett. **92**, 253904 (2004); E.A. Ultanir *et al.*, Opt. Lett. **29**, 845 (2004); A. V. Yulin, D. V. Skryabin, and P. S. J. Russell, Opt. Exp. **13**, 3529 (2005); O. Egorov, F. Lederer, and K. Staliunas, Opt. Lett. **32**, 2106 (2007); O. Egorov and F. Lederer, Opt. Exp. **16**, 6050 (2008); K. Staliunas *et al.*, Phys. Rev. Lett. **101**, 153903 (2008).
- [30] M. Brambilla *et al.*, Phys. Rev. Lett. **79**, 2042 (1997).
- [31] S. Barland *et al.*, Nature **419**, 699 (2002).
- [32] F. Pedaci *et al.*, Appl. Phys. Lett. **92**, 011101 (2008).
- [33] A. Yulin *et al.*, Phys. Rev. A **78**, 061801(R) (2008).
- [34] Y. Larionova *et al.*, Opt. Lett. **33**, 321 (2008).
- [35] L.A.Lugiato and R.Lefever, Phys. Rev. Lett. **58**, 2209 (1987).
- [36] T. C. H. Liew *et al.*, Phys. Rev. Lett. **101**, 016402 (2008).
- [37] A. Amo *et al.*, Nature **457**, 291 (2009).